

## Investigation of the Bioactive Conformation of Histamine H<sub>3</sub> Receptor Antagonists by the Cyclopropylic Strain-Based Conformational Restriction Strategy

Mizuki Watanabe,<sup>†,‡</sup> Takatsugu Hirokawa,<sup>‡,‡</sup> Takaaki Kobayashi,<sup>†</sup> Akira Yoshida,<sup>§</sup> Yoshihiko Ito,<sup>§</sup> Shizuo Yamada,<sup>§</sup> Naoki Orimoto,<sup>||</sup> Yasundo Yamasaki,<sup>||</sup> Mitsuhiro Arisawa,<sup>†</sup> and Satoshi Shuto<sup>\*,†</sup>

<sup>†</sup>Faculty of Pharmaceutical Sciences, Hokkaido University, Kita-12, Nishi-6, Kita-ku, Sapporo 060-0812, Japan, <sup>‡</sup>Computational Biology Research Center, National Institute of Advanced Industrial Science and Technology, Aomi, Koutou-ku, Tokyo 135-0064, Japan, <sup>§</sup>Department of Pharmacokinetics and Pharmacodynamics and Global Center of Excellence (COE), School of Pharmaceutical Sciences, University of Shizuoka, Yada, Shizuoka 422-8526, Japan, and <sup>||</sup>Hanno Research Center, Taiho Pharmaceutical Co. Ltd., Misugidai, Hanno 357-8527, Japan. <sup>‡</sup>M.W. and T.H. contributed equally to this work.

Received December 15, 2009

We previously identified the highly potent histamine H<sub>3</sub> receptor antagonists (1*R*,2*S*)-2-[2-(4-chlorobenzylamino)ethyl]-1-(1*H*-imidazol-4-yl)cyclopropane (**1**) and its enantiomer *ent*-**1**. Although the conformations of **1** and *ent*-**1** are restricted by the central cyclopropane ring, the 2-(4-chlorobenzylamino)ethyl side chain essential for the H<sub>3</sub> receptor binding may somewhat freely rotate. To investigate the bioactive conformation, the 1'-ethyl-substituted derivatives **2a** and **2b** and their enantiomers *ent*-**2a** and *ent*-**2b** were designed as side chain conformation-restricted analogues of **1** and *ent*-**1**, based on the cyclopropylic strain. These compounds were synthesized, and their analysis by NMR and calculations suggested that the side chain moiety was effectively restricted in a *syn*-form or an *anti*-form by the cyclopropylic strain as expected. Pharmacological evaluation and docking simulation showed that the bioactive conformations of **1** and *ent*-**1** appear to be the *syn*-form and the *anti*-form, respectively. Thus, the cyclopropylic strain can be effectively used for conformational restriction of the side chain moiety of cyclopropane compounds.

### Introduction

Attention has been focused on the histamine H<sub>3</sub> receptor, which is a G-protein-coupled receptor (GPCR<sup>q</sup>) distributed mainly in the central nervous system.<sup>1</sup> Antagonists to the H<sub>3</sub> receptor are considered to be potential drugs for various diseases, such as Alzheimer's disease, attention-deficit/hyperactivity disorder (ADHD), schizophrenia, depression, dementia, obesity, and epilepsy.<sup>1b,d,e</sup> As a result, attempts to develop H<sub>3</sub> receptor antagonists have led to the identification of potent H<sub>3</sub> receptor ligands,<sup>1b–f</sup> some of which are shown in Figure 1.

GPCRs are considered to be major targets for drug development.<sup>2</sup> Indeed, it is estimated that over 50% of all modern drugs are targeted at GPCRs.<sup>2a</sup> However, because of the membranous nature of these proteins and their very low natural abundance, structural analysis of GPCRs is difficult. In fact, until the most recent resolution of the adrenergic  $\beta_2$  receptor structures,<sup>3</sup> the only high-resolution structure of a GPCR available had been that of bovine rhodopsin.<sup>2b</sup> One obvious drawback in drug development targeting GPCRs is therefore poor structural data on these proteins.

Conformational restriction of neurotransmitters may improve the specific binding to one of the receptor subtypes.<sup>4</sup> In conformationally restricted analogues highly selectively bound to the target receptor, the functional groups essential for the receptor binding must assume a special arrangement superimposed on the bioactive conformation, in which these functional groups effectively interact with certain amino acid residues in the binding pocket of the receptor. The major problem in designing conformationally restricted analogues specific for a receptor subtype is that the conformation of the conformationally flexible lead compound that binds to the target subtype, i.e., the bioactive conformation, is often unknown. This is mainly because structural analysis of membrane-bound proteins is tremendously difficult,<sup>2</sup> compared with that of proteins soluble in blood or cytosol. Thus, a method for effectively identifying compounds targeting GPCRs, which do not involve structural data, would be highly useful in drug development. Consequently, we have devised a stereochemical diversity-oriented conformational restriction strategy to develop compounds that bind selectively to target proteins of unknown structure such as GPCRs.<sup>5</sup> In this strategy, the versatile chiral cyclopropane units with different stereochemistries (Figure 2)<sup>5a</sup> are effectively used as the key tool for the design and synthesis of a series of conformationally restricted analogues with stereochemical diversity.<sup>5</sup>

On the basis of this stereochemical diversity-oriented strategy, we recently designed and synthesized a series of conformationally restricted analogues of histamine, as shown in Figure 2, with different stereochemistries.<sup>5</sup> In these analogues, the imidazole

\*To whom correspondence should be addressed. Phone and fax: +81-11-706-3769. E-mail: shu@pharm.hokudai.ac.jp.

<sup>a</sup>Abbreviations: ADHD, attention-deficit/hyperactivity disorder; EBNA, Epstein–Barr virus nuclear antigen-1; GPCR, G-protein-coupled receptor; GPCRDB, G-protein-coupled receptors data bank; IFD, induced fit docking; OPLS-AA, optimized potentials for liquid simulations-all-atom; PGME, phenylglycine methyl ester; XP, extra-precision.

and the amino groups are located in a variety of spatial arrangements because of the conformational restriction. Some of these analogues were shown to be potent H<sub>3</sub> receptor ligands, and a conformationally restricted analogue **1** with a (1*R*)-*trans*-cyclopropane structure and its enantiomer *ent-1* (Figure 3) were identified as highly potent H<sub>3</sub> receptor antagonists.<sup>5c</sup>

With these results in hand, we thought that, based on the structures of **1** and *ent-1*, identification of the bioactive conformation for the H<sub>3</sub> receptor antagonists might be possible. If indeed this could be accomplished, the information obtained would be useful in designing further effective compounds. Although the conformation of **1** is restricted by the (1*R*)-*trans*-cyclopropane structure, the spatial arrangement of the basic nitrogen of the side chain, which seems to be essential for activity, would be somewhat flexible. Therefore, we decided to restrict the side chain conformation by the cyclopropyl strain-based method,<sup>6,7</sup> a detail of which is described below, to identify the bioactive conformation. During our study, X-ray crystallographic structures of adrenergic β<sub>2</sub> receptors were reported,<sup>3</sup> and as a consequence, the H<sub>3</sub> receptor model using the structural data of a β<sub>2</sub> receptor was constructed and used for investigating the binding conformation of the conformationally restricted analogues.

In this report, we describe the design, synthesis, pharmacological effects, and receptor modeling studies of the cyclopropyl strain-based conformationally restricted analogues **2a** and **2b** and their enantiomers *ent-2a* and *ent-2b* (Figure 3) for the identification of their bioactive conformations.

## Results and Discussion

**Cyclopropyl Strain-Based Design of the Conformationally Restricted Analogues.** Because of its small and rigid ring

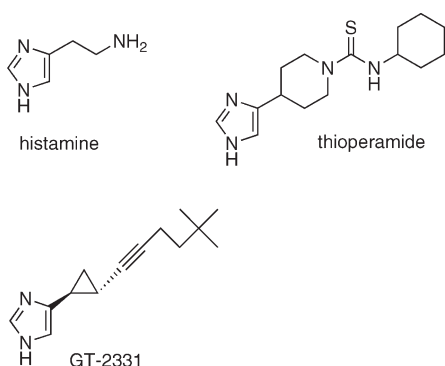


Figure 1. Histamine and representative H<sub>3</sub> receptor ligands.

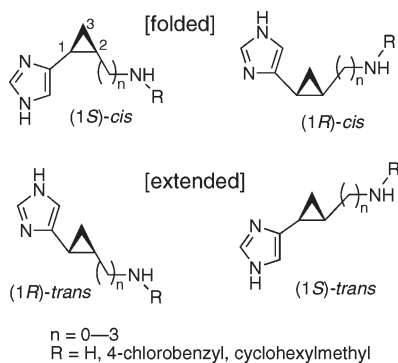


Figure 2. A series of conformationally restricted analogues of histamine with stereochemical diversity synthesized from the chiral cyclopropane units.

structure, cyclopropane is effective in restricting the conformation of a molecule without changing the chemical and physical properties of the lead compound.<sup>8</sup> A characteristic structural feature of cyclopropane is that *cis*-oriented adjacent substituents on the ring exert significant mutual steric repulsion because they are fixed in the eclipsed orientation, which we previously termed “cyclopropyl strain”.<sup>7</sup> Consequently, conformation of the substituents on a cyclopropane can be restricted so that the steric repulsion due to the strain is minimal, as indicated in Figure 4.

Considering that the basic amino function of the H<sub>3</sub> receptor antagonist **1** is likely to be important for the H<sub>3</sub> receptor binding, the conformation of the side chain would significantly affect the activity of the compound. While the cyclopropyl-C1' (C2–C1') bond may freely rotate somewhat, the rotation can be restricted by the cyclopropyl strain. Therefore, the two conformers **A** (*syn*, the C-3 of the cyclopropane “up”/the benzylaminomethyl “up”) and **C** (*anti*, the C-3 of the cyclopropane “up”/the benzylaminomethyl “down”) would be preferable to conformer

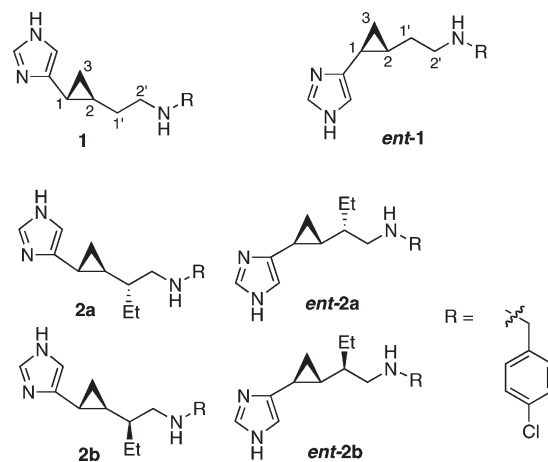


Figure 3. Previously synthesized H<sub>3</sub> receptor antagonists **1** and *ent-1* and their side chain conformationally restricted analogues newly designed.

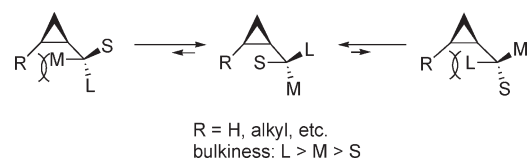
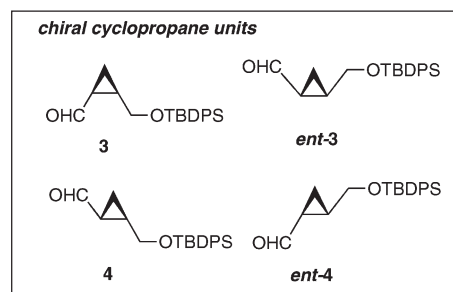
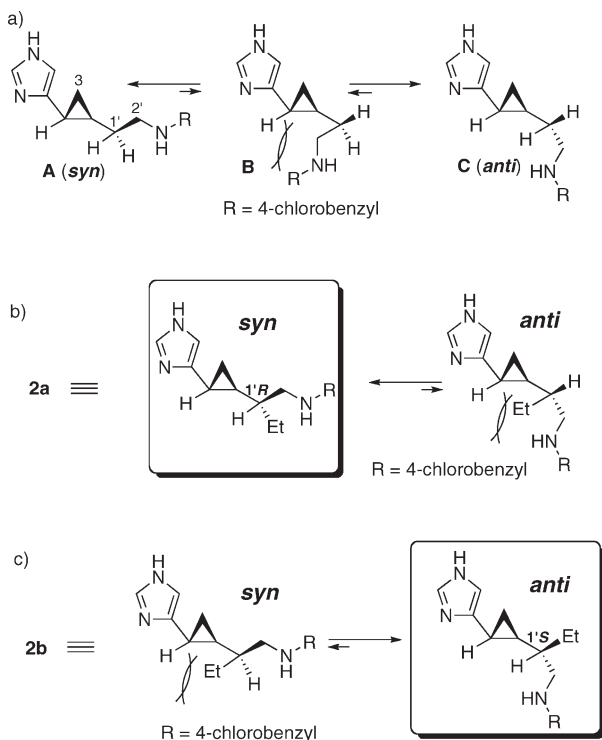
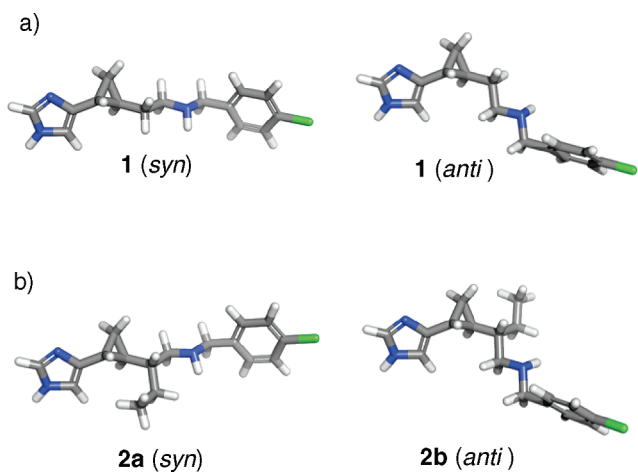


Figure 4. Cyclopropyl strain-based conformational restriction.





**Figure 5.** Presumed stable conformations of **1** (a), **2a** (b), and **2b** (c).

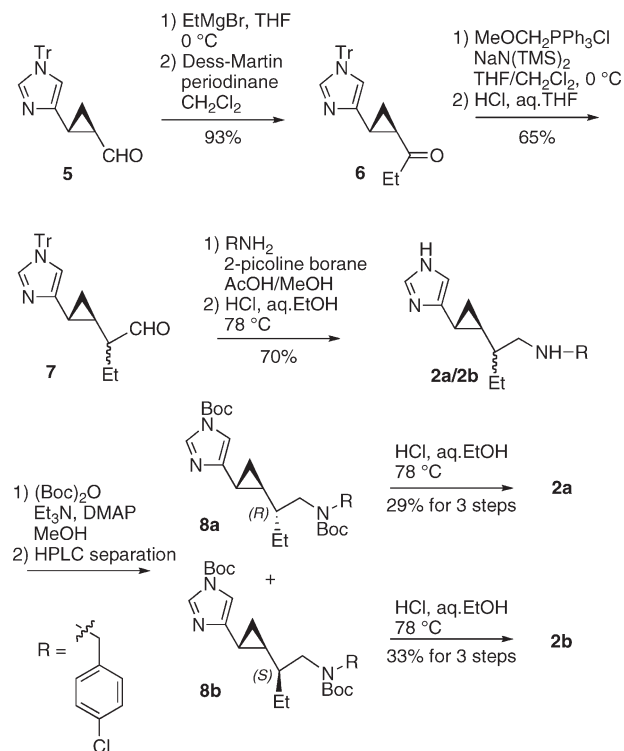


**Figure 6.** Stable structures of the conformationally restricted analogues in the gas phase obtained by the conformational search program in MacroModel: (a) the *syn*-conformer and the *anti*-conformer for **1**; (b) the *syn*-conformer for **2a** and the *anti*-conformer for **2b**.

**B** in compound **1** because of the significant steric repulsion for the adjacent cis-proton in conformer **B**, as shown in Figure 5a.

The conformation of **1** was analyzed by molecular mechanics calculations with MacroModel (Schrödinger, LLC). As a result, as shown in Figure 6a, two significantly stable structures were obtained, which correspond to the *syn*- and the *anti*-conformers in Figure 5a, respectively. The two conformers are nearly equally stable, while the *anti*-conformer is only 0.31 kcal/mol more stable than the *syn*-conformer. Thus, the results of calculations are in accord with the above hypothesis on the conformation of **1**, which suggests that the bioactive conformation may be analogous to either the *syn*-conformer or the *anti*-conformer.

### Scheme 1



We designed the 1'-ethyl-substituted derivatives **2a** and **2b** (Figure 3) as side chain conformation-restricted analogues of **1**. Introducing an ethyl group into the  $\alpha$ -position of the amino function of **1** would prevent the rotation of the side chain moiety by restricting the conformation due to the cyclopropylic strain, i.e., the steric repulsion for the adjacent eclipsed proton. Accordingly, depending on the configuration at the C1' position, the conformation of the compounds can be restricted; the *syn*-conformer would be quite stable in **2a** of the 1'*R*-configuration (Figure 5b); conversely, the *anti*-conformer would be stable in **2b** of the 1'*S*-configuration (Figure 5c).

Thus, while cyclopropane is very effective for conformational restriction of conformationally flexible lead compounds, the cyclopropylic strain-based conformational restriction makes the more precise conformational restriction of cyclopropane compounds possible, especially in the side chain moiety.

**Synthesis.** Although much effort has been devoted to developing practical methods for preparing chiral cyclopropanes, synthesis of cyclopropane derivatives with the desired stereochemistry is often troublesome.<sup>9</sup> The chiral cyclopropane units (Figure 2), which are composed of four stereoisomeric cyclopropane derivatives bearing two adjacent carbon substituents in a cis or a trans relationship, are useful for the synthesis of various cyclopropane compounds, particularly for those with stereochemical diversity.<sup>5</sup>

As summarized in Scheme 1, the target compounds **2a** and **2b** were synthesized from an imidazolylcyclopropanecarboxaldehyde **5** with the (1*R*,2*R*)-structure, which was prepared from the unit **4** by our previous method.<sup>5a</sup> Treatment of **5** with EtMgBr in THF gave a diastereomeric mixture of the addition products, the Dess–Martin oxidation of which afforded the corresponding ketone **6**. Wittig reaction of **6** with MeOCH<sub>2</sub>-PPh<sub>3</sub>Cl/NaN(TMS)<sub>2</sub> followed by acidic treatment gave the

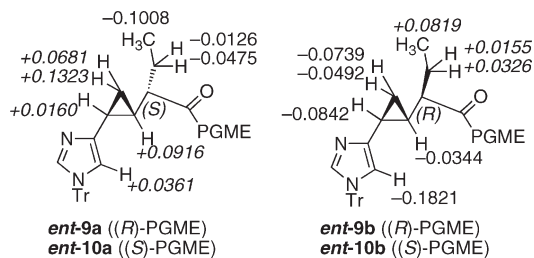


**Figure 7.** Determination of the 1'-configurations based on the  $\Delta\delta$  values (DMSO- $d_6$ , 500 MHz) of the (*R*)- and (*S*)-PGME amides.

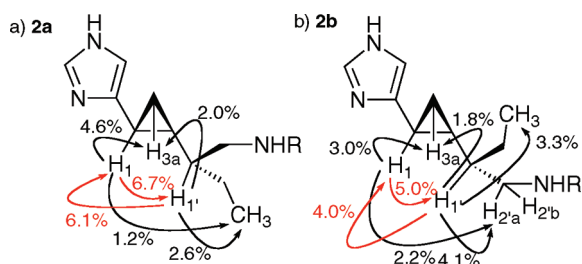


**Figure 8.** NOE data of **2a** and **2b** in D<sub>2</sub>O.

aldehyde **7** as an inseparable diastereomeric mixture (dr, 1/1.1). Reductive amination of **7** with 4-chlorobenzylamine and 2-picoline borane in AcOH/MeOH and subsequent acidic removal of the trityl group of the product gave the desired cyclopropylic strain-based conformationally restricted analogues **2a** and **2b** as a diastereomeric mixture. Although the diastereomers were inseparable at this stage, they were successfully separated by HPLC after protection of the imidazole and amino nitrogens with Boc groups to give the diastereomerically pure **8a** and **8b**, respectively. Acidic removal of the Boc groups of **8a** and **8b** afforded the target (1'*R*)-product **2a** and the (1'*S*)-product **2b**, respectively. The enantiomers **ent-2a** and **ent-2b** were similarly synthesized from **ent-5**.

The 1'-configurations of the cyclopropylic strain-based conformationally restricted analogues synthesized were determined by the phenylglycine methyl ester (PGME) method<sup>10</sup> by converting diastereomerically pure **ent-7a** and **ent-7b** into the corresponding (*R*)-PGME amides **ent-9a** and **ent-9b** and (*S*)-PGME amides **ent-10a** and **ent-10b**,<sup>11</sup> respectively, as shown in Figure 7.

**Conformational Analysis by NMR and Calculations.** Stable structures of the conformationally restricted analogues **2a** and **2b** were investigated by NOE experiments (Figure 8). Irradiations of H-1' of **2a** or **2b** gave NOEs with both H-1 and H-3a oriented cis to H-1. Especially significant NOEs were observed between H-1' and H-1 in both **2a** and **2b**, which show that the side chain conformation of the two compounds seems to be actually restricted by the cyclopropylic strain. When H-1 on the cyclopropane ring of the (1'*R*)-diastereomer **2a** was irradiated, an NOE with the terminal methyl protons of the ethyl group was observed to suggest that it is restricted to the *syn*-form as expected. On the other hand, during irradiation of H-1 of the (1'*S*)-diastereomer **2b**, an NOE was observed with the methylene proton H-2'a adjacent to the basic nitrogen to demonstrate that it is in the *anti*-form, as expected.

The conformations of **2a** and **2b** were also examined by calculations with MacroModel. As shown in Figure 6b, the most stable structures obtained by the calculations were the *syn*-form for **2a** and the *anti*-form for **2b**, respectively.

**Table 1.** Effects of Compounds on the Human H<sub>3</sub> Receptor Subtype<sup>a</sup>

compd	configuration	conformation	inhibition (%) <sup>b</sup>	K <sub>i</sub> (nM)
<b>2a</b>	(1 <i>R</i> )- <i>trans</i> -(1' <i>R</i> )	<i>syn</i>	95	19.8 ± 2.8
<b>2b</b>	(1 <i>R</i> )- <i>trans</i> -(1' <i>S</i> )	<i>anti</i>	73	129 ± 6.0
<b>1</b>	(1 <i>R</i> )- <i>trans</i>	<i>syn/anti</i>	100	8.4 ± 1.5 <sup>c</sup>
<b>ent-2a</b>	(1 <i>S</i> )- <i>trans</i> -(1' <i>S</i> )	<i>syn</i>	96	63.0 ± 6.1
<b>ent-2b</b>	(1 <i>S</i> )- <i>trans</i> -(1' <i>R</i> )	<i>anti</i>	88	6.7 ± 0.4
<b>ent-1</b>	(1 <i>S</i> )- <i>trans</i>	<i>syn/anti</i>	100	3.6 ± 0.4 <sup>c</sup>
thioperamide			98	51.1 ± 3.8 <sup>c</sup>

<sup>a</sup> Assays were carried out with 293-EBNA cells or cell membranes expressing the human H<sub>3</sub> receptor subtype. <sup>b</sup> Inhibitory effect of compound (10<sup>-4</sup> M) on the agonistic activity of histamine (10<sup>-6</sup> M). <sup>c</sup> Data were taken from ref 5c.

The calculated energy barriers for the rotation of the C2–C1' bond between the *syn*-form and the *anti*-form are significant, which are 5.22 kcal/mol for **2a** and 5.55 kcal/mol for **2b**, respectively.

Thus, these conformational analyses suggested that the cyclopropylic strain-based conformational restriction seems to work effectively in **2a** and **2b**, and therefore, pharmacological evaluations of these compounds would help to identify the bioactive conformation.

**Pharmacological Effects.** Effects of compounds on the H<sub>3</sub> receptor were investigated by luciferase reporter gene assay. The human histamine receptor subtypes were individually expressed in 293-Epstein–Barr virus nuclear antigen-1 (EBNA) cells according to the previously reported method,<sup>5b</sup> and the function of the compounds on these receptors expressed on the cells was evaluated. None of the newly synthesized compounds **2a**, **2b**, **ent-2a**, and **ent-2b** showed any agonistic activity to the H<sub>3</sub> receptor at 10<sup>-5</sup> M (data not shown). On the other hand, all of these compounds inhibited the agonistic effect of histamine to show that they are antagonists of the H<sub>3</sub> receptor as are the parent compounds **1** and **ent-1**, as shown in Table 1.

Binding affinities of compounds **2a**, **2b**, **ent-2a**, and **ent-2b** for the human H<sub>3</sub> receptor subtype using [<sup>3</sup>H]*N*<sup>α</sup>-methylhistamine<sup>5c</sup> were next investigated and were compared with those of their parent compounds **1** and **ent-1** (Table 1). In this system, the well-known H<sub>3</sub> receptor antagonist thioperamide showed a K<sub>i</sub> value of 51.1 nM, and compounds **1** and **ent-1** displayed much higher binding affinity for the human H<sub>3</sub> receptor as shown by the K<sub>i</sub> values of 8.4 and 3.6 nM, respectively.

Although compound **2a**, which is restricted in the *syn*-conformation, showed remarkable binding affinity for the receptor with a K<sub>i</sub> value of 19.8 nM, compound **2b**, restricted in the *anti*-conformation, showed more than 15-fold reduction of potency (K<sub>i</sub> = 129 nM), compared with the parent compound **1**. On the other hand, of the enantiomers **ent-2a** and **ent-2b**, **ent-2b** (K<sub>i</sub> = 6.7 nM), which is restricted in the *anti*-conformation, showed 10-fold higher binding affinity for the human H<sub>3</sub> receptor than the **ent-2a** (K<sub>i</sub> = 63 nM), which is restricted in the *syn*-conformation.

**Docking Simulation by Homology Modeling.** The above conformational analysis and pharmacological results showed that in the diastereomeric pair of **2a** and **2b**, the *syn*-restricted **2a** was more potent than the *anti*-restricted **2b**, while in their enantiomers **ent-2a** and **ent-2b**, the *anti*-restricted **ent-2b** was more potent than the *syn*-restricted **ent-2a**. In order to understand the discrepancy in the conformation–activity relationship between **2a/2b** and **ent-2a/ent-2b**, we planned to perform a docking simulation with a



homology modeling of the H<sub>3</sub> receptor to investigate the binding mode of these cyclopropyl strain-based conformationally restricted analogues in the active site of the H<sub>3</sub> receptor.

Previous studies showed that homology models of H<sub>3</sub> receptor are useful for providing structural insight into the ligand binding mechanism, QSAR analysis, and in silico drug discovery.<sup>13</sup> Furthermore, most recent resolutions of the ligand-binding adrenergic  $\beta_2$  receptor structures<sup>3</sup> give us a chance to generate more accurate three-dimensional models for target GPCRs with a ligand using homology modeling and docking simulation.<sup>14</sup>

Thus, in this study, a three-dimensional model of the H<sub>3</sub> receptor was constructed on the basis of a structural template from the crystal structure of the human  $\beta_2$ -adrenergic GPCR recently reported by Cherezov and co-workers,<sup>3a</sup> and docking simulations of the compounds into the H<sub>3</sub> receptor model were performed with ligand and receptor flexibility.

We constructed a homology model based on the conformationally restricted analogue *ent-2b*, which is the most

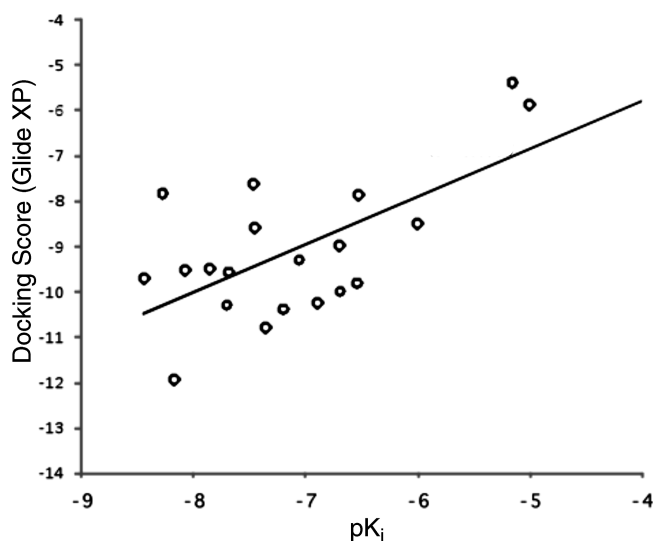


**Figure 9.** Plot of binding score calculated by Glide extrapolation (XP) based on *ent-2b*-bound H<sub>3</sub> receptor model versus experimental binding affinity pK<sub>i</sub> for 20 conformational restriction analogues. The coefficient of determination,  $R^2$ , between binding score and pK<sub>i</sub> was 0.41 for 20 conformational restriction analogues.

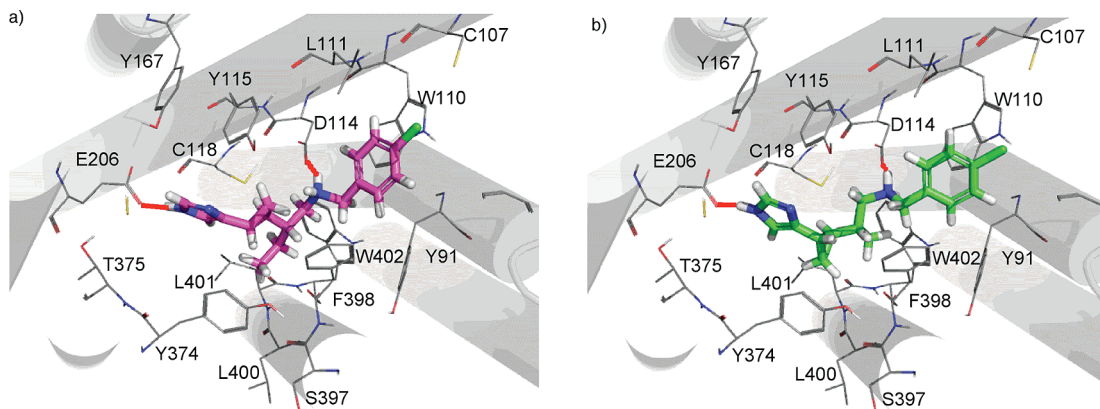


**Figure 10.** Proposed models for **2a** (a) and *ent-2b* (b) binding to the homology model of the H<sub>3</sub> receptor from docking simulation. Receptor residues around the compounds within 4 Å are shown in line representation. Carbon atoms of **2a** and *ent-2b* are shown in magenta and green, respectively. All nonpolar hydrogen atoms of receptor residues are omitted for clarity. Hydrogen bonding and salt bridge to side chain carboxyl group of Glu206 and Asp114 are depicted by red dots.

potent H<sub>3</sub> receptor ligand in this series of the cyclopropane-based conformationally restricted analogues. Using this model, we performed docking simulation with a series of the cyclopropane-based conformationally restricted H<sub>3</sub>-receptor ligands having stereochemical diversity (16 compounds) synthesized previously<sup>5c,12</sup> and also with the four cyclopropyl strain-based conformationally restricted analogues **2a**, **2b**, *ent-2a*, and *ent-2b* synthesized in this study. Correlations between the calculated binding score and the pK<sub>i</sub> were examined. As a result, as shown in Figure 9, a reliable correlation ( $R^2 = 0.41$ ) between binding score and pK<sub>i</sub> was obtained. Consequently, the *ent-2b*-bound H<sub>3</sub> receptor model was also used for further studies.

In order to understand the binding modes of the newly synthesized cyclopropyl strain-based conformationally restricted analogues to the H<sub>3</sub> receptor, docking simulations of **2a** and **2b** and their enantiomers *ent-2b* and *ent-2b* were carried out by using the *ent-2b*-bound model. Figure 10 shows the proposed binding modes of the potent H<sub>3</sub> antagonists **2a** and *ent-2b* to the homology model of the H<sub>3</sub> receptor obtained by the simulation. These compounds are accommodated in the active site concavity formed by TM2, TM3, TM5, TM6, and TM7. The H<sub>3</sub> receptor-binding conformations of **2a** and *ent-2b* are the *syn*-form and the *anti*-form, respectively, as shown in Figures 10 and 11, which are in accord with the stable forms proposed by their conformational analysis by NMR and the calculations described above.

In the obtained binding models shown in Figure 10, the NH of the imidazole ring of both compounds likewise serves as a hydrogen donor and forms a hydrogen bond with an oxygen atom of the side chain carboxyl group of Glu206. Furthermore, the protonated amine in both **2a** and *ent-2b* forms a similar salt bridge with Asp114 in TM3, and the 4-chlorobenzyl group in **2a** and *ent-2b* is observed to make a  $\pi$ - $\pi$  interaction with the indole ring of Trp110 in TM3. Thus, the special positioning of the imidazole moiety and the 4-chlorobenzylamino moiety in **2a** and *ent-2b*, which are likely to be essential for their H<sub>3</sub> receptor binding, is analogous in the active site, and therefore **2a** and *ent-2b* may have a common pharmacophore. As shown in Figure 11a, the imidazole and 4-chlorobenzylamino moieties of **2a** and *ent-2b* can be superimposed, where the two cyclopropane rings orient oppositely, i.e., “up” in **2a** and “down” in *ent-2b*, respectively. This would explain why **2a** and *ent-2b* have a similar potent antagonistic effect on the H<sub>3</sub> receptor, even though the two compounds are conformationally restricted

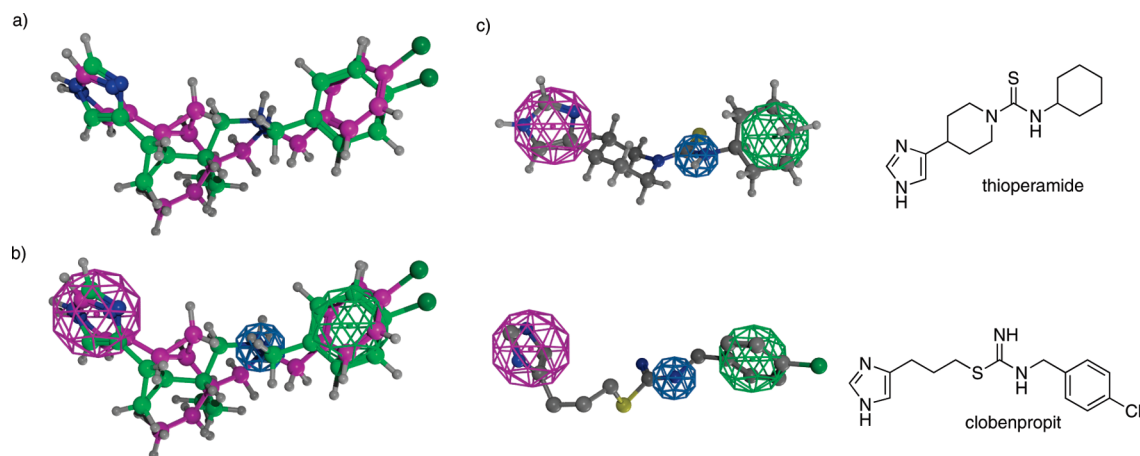


**Figure 11.** Superimposition of the structures of **2a** (magenta) and *ent-2b* (green) binding to the homology model of the H<sub>3</sub> receptor (a). Three-feature pharmacophore model generated for **2a** and *ent-2b* using MOE: hydrogen bond acceptor/donor (magenta feature), hydrogen bond donor/cationic atom (blue feature), and aromatic ring center/hydrophobic region (green feature) (b). Known H<sub>3</sub> receptor ligands are mapped onto the pharmacophore model obtained from **2a** and *ent-2b* (c).

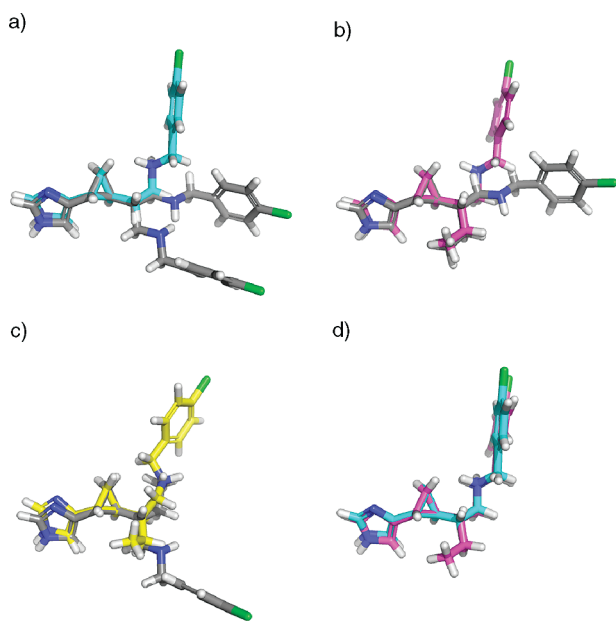


**Figure 12.** Comparison of conformational changes between the stable forms shown in Figure 6 and the bioactive forms proposed by the H<sub>3</sub> receptor-bound model. Shown are the two stable conformations and the bioactive conformations for **1** (a), the stable and the bioactive conformations for **2a** (b) and **2b** (c), and superimposition of the bioactive conformations of **1** and **2a** (d). Carbon atoms of stable conformations for all compounds are shown in gray, and carbon atoms of the bioactive conformations for **1**, **2a**, and **2b** are shown in blue, magenta, and yellow, respectively. All compounds are aligned on the cyclopropane ring.

differently, i.e., the *syn*-form and the *anti*-form, respectively, by the cyclopropylic strain. Figure 11b shows a common pharmacophore model for **2a** and *ent-2b*, and the model effectively fitted in known H<sub>3</sub> receptor ligands,<sup>1</sup> as shown in Figure 11c.

We next examined the possible conformational differences between the stable form and the bioactive form of the compounds, which could significantly affect the binding affinity, based on the proposed receptor-bound model. In Figure 12, the stable conformations of **1** and its conformationally restricted analogues **2a** and **2b** based on NMR and calculation analysis are superimposed on their receptor-bound (bioactive) conformations by the receptor modeling

simulations. As shown in Figure 12a, the bioactive conformation of **1** is in accord with the *syn*-form of the two stable *syn*- and *anti*-conformations. Figure 12b shows that the stable *syn*-form of **2a** is almost identical with the bioactive conformation in **2a**, which would make it highly potent. On the other hand, in **2b**, the bioactive conformation is the *syn*-form similar to **1** and **2a**, while **2b** itself is stable in the *anti*-form (Figure 12c). Thus, because of the entropic cost for the conformational change from the stable *anti*-form into the bioactive *syn*-form in its binding to the H<sub>3</sub> receptor, the binding affinity of **2b** for the H<sub>3</sub> receptor is significantly decreased. In Figure 12d, the receptor-bound conformations of **1** and **2a** were superimposed, showing that their bioactive conformations are the same. These results suggested that the cyclopropylic strain-based conformational restriction worked effectively as expected.

As described, we identified the potent H<sub>3</sub> receptor antagonists **1** and *ent-1* by the stereochemical diversity-oriented conformational restriction method with chiral cyclopropane units as shown in Figure 2. Their bioactive conformations and a pharmacophore model were further elaborated by the cyclopropylic strain-based conformational restriction method. These results showed that the combinational use of the stereochemical diversity-oriented and the cyclopropylic strain-based conformational restriction methods seems to be an effective strategy for developing significantly active compounds and also for identifying their bioactive conformations, especially in cases where the structural data of the target biomolecule are lacking or poorly documented. In these studies, simulations with homology modeling of the target biomolecule can be effective. This is due to the fact that a series of cyclopropane analogues and also cyclopropane strain-based conformationally restricted analogues are suitable for validating the homology models, since these consist of compounds having diversity not only in their conformation, i.e., three-dimensional structure, but also in their binding affinity for the target.

## Conclusion

In order to clarify the bioactive conformation of the previously developed H<sub>3</sub> receptor antagonists **1** and *ent-1*, the 1'-ethyl-substituted derivatives **2a** and **2b** and their enantiomers

**ent-2a** and **ent-2b** were designed as side chain conformation-restricted analogues of **1** and **ent-1**, based on the cyclopropylic strain, and were synthesized from the versatile chiral cyclopropane units. Conformational analysis, pharmacological evaluation, and docking simulation of the compounds showed that the bioactive conformations of **1** and **ent-1** seem to be the *syn*-form and the *anti*-form, respectively. On the basis of these results, a common pharmacophore for the compounds was obtained. These results suggest that the cyclopropylic strain-based strategy can be effectively used for precise conformational restriction of the side chain moiety and bioactive conformation analysis of cyclopropane compounds.

## Experimental Section

Chemical shifts are reported in ppm downfield from tetramethylsilane. Thin-layer chromatography was done on Merck coated plate 60F<sub>254</sub>. Silica gel chromatography was done on silica gel 5715 (Merck) or NH silica gel (Chromatorex, Fuji Silysia Chemical Ltd.). Reactions were carried out under an argon atmosphere. Estimated purity of all of the final compounds by combustion analysis was always at least 95%.

**(1R,2R)-2-(1-Oxopropyl)-1-(1-triphenylmethyl-1H-imidazol-4-yl)cyclopropane (6)**. To a solution of **5**<sup>5a</sup> (238 mg, 0.629 mmol) in THF (5.0 mL) was added EtMgBr (0.91 M in THF, 830  $\mu$ L, 0.755 mmol) at 0 °C, and the mixture was stirred at the same temperature for 1 h. After addition of aqueous saturated NH<sub>4</sub>Cl, the solvent was evaporated, and the residue was partitioned between AcOEt and aqueous NH<sub>4</sub>Cl. The organic layer was washed with brine, dried (Na<sub>2</sub>SO<sub>4</sub>), and evaporated. To a solution of the residue in CH<sub>2</sub>Cl<sub>2</sub> (5 mL) was added Dess–Martin periodinane (320 mg, 0.755 mmol) at room temperature, and the mixture was stirred at the same temperature for 1 h. To the reaction mixture was added a mixture of aqueous saturated NaHCO<sub>3</sub> and aqueous saturated Na<sub>2</sub>S<sub>2</sub>O<sub>3</sub> (3/1, 12 mL) at room temperature, and the resulting mixture was vigorously stirred at the same temperature for 10 min. The resulting solution was extracted with AcOEt, and the organic layer was washed with aqueous saturated NaHCO<sub>3</sub>, brine, dried (Na<sub>2</sub>SO<sub>4</sub>), and evaporated. The residue was purified by silica gel column chromatography (20–33% AcOEt in hexane) to give **6** (239 mg, 93%) as a white amorphous solid:  $[\alpha]_D^{19}$  –217.3 (*c* 0.86, CHCl<sub>3</sub>); <sup>1</sup>H NMR (400 MHz, CDCl<sub>3</sub>)  $\delta$  1.07 (3 H, t, *J* = 7.3 Hz, CH<sub>3</sub>CH<sub>2</sub>), 1.44 (1 H, m, H-3a), 1.50 (1 H, m, H-3b), 2.38 (2 H, m, H-1 and H-2), 2.61 (2 H, q, *J* = 7.3 Hz, CH<sub>3</sub>CH<sub>2</sub>), 6.64 (1 H, d, *J* = 1.2 Hz, imidazolyl), 7.11–7.14 (6 H, m, aromatic), 7.28 (1 H, s, imidazolyl), 7.32–7.34 (9 H, m, aromatic); <sup>13</sup>C NMR (100 MHz, CDCl<sub>3</sub>)  $\delta$  7.96, 18.0, 22.5, 30.1, 37.0, 75.2, 118.0, 127.9, 129.7, 138.4, 138.4, 139.9, 142.2, 209.9; LRMS (EI) *m/z* 406 (M<sup>+</sup>); HRMS (EI) calcd for C<sub>28</sub>H<sub>26</sub>N<sub>2</sub>O 406.2045, found 406.2050 (M<sup>+</sup>). Anal. (C<sub>28</sub>H<sub>26</sub>N<sub>2</sub>O) C, H, N.

**(1R,2R)-2-(1-Formylpropyl)-1-(1-triphenylmethyl-1H-imidazol-4-yl)cyclopropane (7)**. To a suspension of MeOCH<sub>2</sub>PPh<sub>3</sub>Cl (608 mg, 1.77 mmol) in THF (5.0 mL) was added NaN(Si(CH<sub>3</sub>)<sub>3</sub>)<sub>2</sub> (~1.9 M in THF, 800  $\mu$ L, 1.52 mmol) at 0 °C, and the mixture was stirred at the same temperature for 15 min. To the resulting solution was added a solution of **6** (206 mg, 0.507 mmol) in CH<sub>2</sub>Cl<sub>2</sub> (2.0 mL) at 0 °C, and the reaction mixture was stirred at the same temperature for 2 h. After addition of aqueous saturated NH<sub>4</sub>Cl, the solvent was evaporated, and the residue was partitioned between AcOEt and aqueous NH<sub>4</sub>Cl. The organic layer was washed with brine, dried (Na<sub>2</sub>SO<sub>4</sub>), and evaporated. The residue was purified by silica gel column chromatography (30% AcOEt in hexane) to give the enol ether product (151 mg) as a light-yellow solid. To a solution of the product in THF (10 mL) was added aqueous HCl (12 M, 5.0 mL), and the mixture was vigorously stirred at room temperature for 10 s. Immediately, the mixture was poured into aqueous saturated NaHCO<sub>3</sub> (100 mL). Then the resulting solution was extracted with AcOEt.

The organic layer was washed with aqueous saturated NaHCO<sub>3</sub>, brine, dried (Na<sub>2</sub>SO<sub>4</sub>), and evaporated. The residue was purified by silica gel column chromatography (25–40% AcOEt in hexane) to give **7** (diastereomixture, 138 mg, 65%) as a yellow amorphous solid: HRMS (EI) calcd for C<sub>29</sub>H<sub>28</sub>N<sub>2</sub>O 420.2202, found 420.2200 (M<sup>+</sup>).

**(1R,2S)-2-[1-Ethyl-2-(4-chlorobenzylamino)ethyl]-1-(1H-imidazol-4-yl)cyclopropane (2a/2b)**. To a solution of **7** (112 mg, 0.266 mmol) and 4-chlorobenzylamine (35  $\mu$ L, 0.28 mmol) in MeOH/AcOH (10/1, 2.2 mL) was added 2-picolineborane (30 mg, 0.28 mmol) at room temperature, and the mixture was stirred at the same temperature for 12 h. After evaporation of the solvent, a solution of the residue in aqueous HCl (4 M, 4.0 mL) was stirred at 0 °C for 20 min, and then the mixture was neutralized with Na<sub>2</sub>CO<sub>3</sub>. The mixture was partitioned between CH<sub>2</sub>Cl<sub>2</sub> and aqueous saturated NaHCO<sub>3</sub>, and the organic layer was washed with brine, dried (Na<sub>2</sub>SO<sub>4</sub>), and evaporated. The residue was purified by neutral silica gel column chromatography (0–10% MeOH in CHCl<sub>3</sub>) to give amine product (diastereomixture, 108 mg) as a light-yellow amorphous solid. To a solution of amine (108 mg) in EtOH (1.0 mL) was added aqueous HCl (2 M, 1.0 mL), and the resulting solution was stirred at 78 °C for 2 h, and then the solvent was evaporated. The residue was partitioned between aqueous HCl (1 M) and CH<sub>2</sub>Cl<sub>2</sub>, and the aqueous layer was neutralized with aqueous NaOH (2 M). The resulting solution was extracted with Et<sub>2</sub>O, and the organic layer was washed with H<sub>2</sub>O, brine, dried (Na<sub>2</sub>SO<sub>4</sub>), and evaporated. The residue was purified by NH silica gel column chromatography (0–5% MeOH in CHCl<sub>3</sub>) to give the diastereomixture of **2a** and **2b** (56 mg, 70%) as a colorless amorphous solid: HRMS (EI) calcd for C<sub>17</sub>H<sub>22</sub>ClN<sub>3</sub> 303.1502, found 303.1500 (M<sup>+</sup>).

**(1R,2S)-2-[(1R)-1-Ethyl-2-(4-chlorobenzylamino)ethyl]-1-(1H-imidazol-4-yl)cyclopropane (2a)** and **(1R,2S)-2-[(1S)-1-Ethyl-2-(4-chlorobenzylamino)ethyl]-1-(1H-imidazol-4-yl)cyclopropane (2b)**. A solution of the diastereomixture of **2a** and **2b** (56 mg, 0.15 mmol), Et<sub>3</sub>N (83  $\mu$ L, 0.60 mmol), DMAP (1.8 mg, 0.015 mmol), and (Boc)<sub>2</sub>O (130 mg, 0.60 mmol) in MeOH (1 mL) was stirred at room temperature for 16 h. After evaporation of the solvent, the residue was partitioned between AcOEt and H<sub>2</sub>O, and the organic layer was washed with brine, dried (Na<sub>2</sub>SO<sub>4</sub>), and evaporated. The residue was separated by HPLC (28% AcOEt in hexane, 13 mL/min, room temperature, 253 nm) with Mightysil Si 60 (0.25 cm  $\times$  20 cm, Kanto Chemical Co.) to give **8a** (24 mg, a colorless amorphous solid) and **8b** (26 mg, a colorless amorphous solid). Each compound was dissolved in EtOH (1.5 mL)/aqueous HCl (4 M, 0.5 mL), and the mixture was stirred at 78 °C for 2 h. After the mixture was concentrated and dried in vacuo, the residue was purified by NH silica gel column chromatography (0–10% MeOH in CHCl<sub>3</sub>) to give **2a** (12 mg, 29% for three steps, a colorless amorphous solid) or **2b** (14 mg, 33% for three steps, a colorless amorphous solid) as a free amine.

**2a**: <sup>1</sup>H NMR (400 MHz, CDCl<sub>3</sub>)  $\delta$  0.76 (1 H, m, H-3a), 0.87–0.96 (6 H, m, H-3b and H-1' and H-2 and CH<sub>3</sub>CH<sub>2</sub>), 1.45 (1 H, m, CH<sub>3</sub>CH<sub>2</sub>), 1.54 (1 H, m, CH<sub>3</sub>CH<sub>2</sub>), 1.64 (1 H, m, H-1), 2.65 (2 H, dd, *J* = 5.0, 12.0 Hz, H-2'), 3.77 (2 H, s, –CH<sub>2</sub>Ph), 6.63 (1 H, s, imidazolyl), 7.27 (4 H, dd, *J* = 8.0, 8.6 Hz, aromatic), 7.48 (1 H, s, imidazolyl); <sup>13</sup>C NMR (100 MHz, CDCl<sub>3</sub>)  $\delta$  12.0, 13.1, 14.6, 24.7, 26.3, 44.8, 53.8, 53.8, 128.7, 129.6, 132.8, 134.4, 139.2; HRMS (EI) calcd for C<sub>17</sub>H<sub>22</sub>ClN<sub>3</sub> 303.1502, found 303.1501 (M<sup>+</sup>).

The free amine **2a** (12 mg) was dissolved in aqueous HCl (4 M), and the solvent was then evaporated. The residue was triturated with Et<sub>2</sub>O to give **2a** dihydrochloride (15 mg, a white amorphous solid):  $[\alpha]_D^{21}$  –20.5 (*c* 0.81, MeOH); <sup>1</sup>H NMR (400 MHz, D<sub>2</sub>O)  $\delta$  0.89 (3 H, t, *J* = 7.5 Hz, CH<sub>3</sub>CH<sub>2</sub>), 0.93 (1 H, m, H-3a), 0.98–1.06 (2 H, m, H-2 and H-3b), 1.22 (1 H, m, H-1'), 1.54 (2 H, m, CH<sub>3</sub>CH<sub>2</sub>), 1.88 (1 H, m, H-1), 3.11 (2 H, dd, *J* = 1.8, 7.1 Hz, H-2'), 4.20 (1 H, d, *J* = 13.6 Hz, –CH<sub>2</sub>Ph), 4.26 (1 H, d, *J* = 13.6 Hz,



-CH<sub>2</sub>Ph), 7.10 (1 H, s, imidazolyl), 7.46 (4 H, dd,  $J = 8.6, 8.6$  Hz, aromatic), 8.44 (1 H, d,  $J = 1.4$  Hz, imidazolyl); LRMS (EI)  $m/z$  303 ((M - 2HCl)<sup>+</sup>). Anal. (C<sub>17</sub>H<sub>24</sub>Cl<sub>3</sub>N<sub>3</sub>) C, H, N.

**2b**: <sup>1</sup>H NMR (400 MHz, CDCl<sub>3</sub>)  $\delta$  0.72 (1 H, m, H-3a), 0.81 (1 H, m, H-3b), 0.93–0.99 (5 H, m, H-1' and H-2 and CH<sub>3</sub>CH<sub>2</sub>-), 1.47 (2 H, m, CH<sub>3</sub>CH<sub>2</sub>-), 1.64 (1 H, m, H-1), 2.64 (1 H, dd,  $J = 7.4, 11.4$  Hz, H-2'), 2.75 (1 H, dd,  $J = 5.7, 11.4$  Hz, H-2'), 3.74 (1 H, d,  $J = 13.3$  Hz, -CH<sub>2</sub>Ph), 3.78 (1 H, d,  $J = 13.3$  Hz, -CH<sub>2</sub>Ph), 6.67 (1 H, s, imidazolyl), 7.22 (2 H, d,  $J = 8.6$  Hz, aromatic), 7.26 (2 H, d,  $J = 8.6$  Hz, aromatic), 7.44 (1 H, s, imidazolyl); <sup>13</sup>C NMR (100 MHz, CDCl<sub>3</sub>)  $\delta$  11.8, 12.5, 14.6, 24.9, 26.4, 44.8, 53.8, 54.4, 128.8, 129.7, 132.9, 134.5, 139.1; LRMS (EI)  $m/z$  303 (M<sup>+</sup>); HRMS (EI) calcd for C<sub>17</sub>H<sub>22</sub>ClN<sub>3</sub> 303.1502, found 303.1509 (M<sup>+</sup>).

The free amine **2b** (14 mg) was dissolved in aqueous HCl (4 M), and the solvent was then evaporated. The residue was triturated with Et<sub>2</sub>O to give **2b** dihydrochloride (17 mg, a white amorphous solid): [ $\alpha$ ]<sub>D</sub><sup>21</sup> -64.5 ( $c$  1.23, MeOH); <sup>1</sup>H NMR (400 MHz, D<sub>2</sub>O)  $\delta$  0.92 (3 H, t,  $J = 7.2$  Hz, CH<sub>3</sub>CH<sub>2</sub>-), 1.05 (2 H, m, H-3), 1.09 (1 H, m, H-2), 1.23 (1 H, m, H-1'), 1.43–1.60 (2 H, m, CH<sub>3</sub>CH<sub>2</sub>-), 1.74 (1 H, m, H-1), 3.12 (1 H, dd,  $J = 7.4, 13.1$  Hz, H-2a'), 3.19 (1 H, dd,  $J = 5.0, 13.1$  Hz, H-2b'), 4.13 (1 H, d,  $J = 13.6$  Hz, -CH<sub>2</sub>Ph), 4.26 (1 H, d,  $J = 13.6$  Hz, -CH<sub>2</sub>Ph), 6.97 (1 H, s, imidazolyl), 7.39 (4 H, s, aromatic), 8.46 (1 H, d,  $J = 1.4$  Hz, imidazolyl); LRMS (EI)  $m/z$  303 ((M-2HCl)<sup>+</sup>). Anal. (C<sub>17</sub>H<sub>24</sub>Cl<sub>3</sub>N<sub>3</sub>) C, H, N.

**(1S,2S)-2-(1-Oxopropyl)-1-(1-triphenylmethyl-1H-imidazol-4-yl)cyclopropane (ent-6)**. Compound **ent-6** (173 mg, 85%, a white amorphous solid) was prepared from **ent-5** (190 mg, 0.50 mmol) as described for the preparation of **6**: [ $\alpha$ ]<sub>D</sub><sup>20</sup> +232.1 ( $c$  1.03, CHCl<sub>3</sub>); HRMS (EI) calcd for C<sub>28</sub>H<sub>26</sub>N<sub>2</sub>O 406.2045, found 406.2044 (M<sup>+</sup>). Anal. (C<sub>28</sub>H<sub>26</sub>N<sub>2</sub>O) C, H, N.

**(1S,2S)-2-(1-Formylpropyl)-1-(1-triphenylmethyl-1H-imidazol-4-yl)cyclopropane (ent-7)**. Compound **ent-7** (94 mg, 60%, a white amorphous solid) was prepared from **ent-6** (152 mg, 0.37 mmol) as described for the preparation of **7**: HRMS (EI) calcd for C<sub>29</sub>H<sub>28</sub>N<sub>2</sub>O 420.2202, found 420.2220 (M<sup>+</sup>).

**(1S,2R)-2-[(1S)-1-Ethyl-2-(4-chlorobenzylamino)ethyl]-1-(1H-imidazol-4-yl)cyclopropane (ent-2a)**. Compound **ent-2a** (10 mg, 30%, a white amorphous solid) was prepared from **ent-8** (35 mg, 0.11 mmol) as described for the preparation of **2a**: HRMS (EI) calcd for C<sub>17</sub>H<sub>22</sub>ClN<sub>3</sub> 303.1502, found 303.1500 (M<sup>+</sup>). The free amine **ent-2a** (10 mg) was dissolved in aqueous HCl (4 M), and the solvent was then evaporated. The residue was triturated with Et<sub>2</sub>O to give **ent-2a** dihydrochloride (13 mg, a white amorphous solid): [ $\alpha$ ]<sub>D</sub><sup>21</sup> +19.9 ( $c$  0.62, MeOH); LRMS (EI)  $m/z$  303 ((M-2HCl)<sup>+</sup>). Anal. (C<sub>17</sub>H<sub>24</sub>Cl<sub>3</sub>N<sub>3</sub>) C, H, N.

**(1S,2R)-2-[(1R)-1-Ethyl-2-(4-chlorobenzylamino)ethyl]-1-(1H-imidazol-4-yl)cyclopropane (ent-2b)**. Compound **ent-2b** (10 mg, 30%, a white amorphous solid) was prepared from **ent-8** (35 mg, 0.11 mmol) as described for the preparation of **2b**: LRMS (EI)  $m/z$  303 (M<sup>+</sup>); HRMS (EI) calcd for C<sub>17</sub>H<sub>22</sub>ClN<sub>3</sub> 303.1502, found 303.1500 (M<sup>+</sup>). The free amine **ent-2b** (10 mg) was dissolved in aqueous HCl (4 M), and the solvent was then evaporated. The residue was triturated with Et<sub>2</sub>O to give **ent-2b** dihydrochloride (13 mg, a white amorphous solid): [ $\alpha$ ]<sub>D</sub><sup>21</sup> +63.2 ( $c$  1.11, MeOH); LRMS (EI)  $m/z$  303 ((M-2HCl)<sup>+</sup>). Anal. (C<sub>17</sub>H<sub>24</sub>Cl<sub>3</sub>N<sub>3</sub>) C, H, N.

**Binding Assay with Human Histamine Receptors.** The assay was performed according to the method described previously.<sup>5c</sup>

**Luciferase Reporter Gene Assay.** The assay was performed according to the method described previously.<sup>5b</sup>

**Homology Modeling of the H<sub>3</sub> Receptor.** The histamine H<sub>3</sub> receptor sequence was aligned with the human  $\beta_2$ -adrenergic receptor sequence<sup>3a</sup> and 40 representative sequences of class A rhodopsin-like amine families (G-protein-coupled receptors data bank (GPCRDB): <http://www.gpcr.org/7tm/>) using the CLUSTAL W (version 1.8) multiple alignment program.<sup>15</sup> The alignment was refined manually on the basis of the compatibility of the amino acid position with the corresponding structure of the

$\beta_2$ -adrenergic receptor. A three-dimensional model of H<sub>3</sub> receptor was constructed using a homology modeling approach incorporated in the program SegMod<sup>16</sup> of GeneMine.<sup>17</sup> Because it is very long and predicted to be disordered, the third intracellular loop was truncated by the five residues leading out of the helix V and the five residues leading into helix VI. The second extracellular loop was modeled without aligning them with those of the  $\beta_2$ -adrenergic receptor.

**Docking Simulation.** Initial coordinates of all compounds were constructed using the Molecular Builder module in Maestro (Schrödinger LLC.). Energy minimization of all compounds was performed using the optimized potentials for liquid simulations-all-atom (OPLS-AA) force field in the LigPrep in the Maestro (Schrödinger LLC.). The homology model of H<sub>3</sub> receptor was refined for docking simulations using the Protein Preparation Wizard within Maestro. This protein preparation procedure involves optimization of contacts by changing hydroxyl group orientations, flipping of Asn and Gln side chains, and selecting His tautomeric states, followed by constrained energy refinement using the OPLS-AA force field. Docking of the compounds into the H<sub>3</sub> receptor model utilized three main steps that take into account several levels of structural flexibility and scoring criteria: (1) molecular modeling of compound bound H<sub>3</sub> receptor model by docking the **ent-2b** molecule, considering both ligand and receptor flexibility, (2) rigid receptor docking of 20 cyclopropane-based conformational restriction analogues<sup>5c</sup> into the active site of **ent-2b** compound bound H<sub>3</sub> receptor model from the previous step, (3) rescoring according to the calculated binding score by Glide extraprecision (XP) score (Schrödinger LLC).

Following are the details of each step. In order to account for both compound and receptor flexibility in the first step, the Glide "Induced Fit Docking (IFD)" protocol (Schrödinger LLC.) was utilized, followed by iteratively combining rigid receptor docking (Glide) and protein remodeling by side chain searching and minimization (Prime) techniques. Hydrogen-bonding constraints between the side chain COO<sup>-</sup> group of Asp114 and Glu206 were introduced because this hydrogen-bonding formation is highly conserved in almost all known complexes of histamine receptor subfamily bound to histamine and to a wide variety of inhibitors. In the protein remodeling stage, all residues within a 14.0 Å radius of each initial docked compound were refined using Prime. Compound was then redocked into the refined receptor structure using Glide in the standard precision (SP) mode. All of the docked structures were then ranked according to GlideScore. After modeling of the compound-H<sub>3</sub> receptor complex using the IFD protocol, grid generation and rigid receptor docking of the 20 cyclopropane-based conformational restriction analogues using Glide (SP mode) were carried out, using the hydrogen bonding constraint to connect the side chain COO<sup>-</sup> group of Asp114 and Glu206. The best orientation for each docked compound was rescored according to its binding score, which was calculated using the Glide XP Score (Schrödinger LLC).

**Acknowledgment.** This investigation was supported by a Grant-in-Aids for Scientific Research (Grant 21390028) from the Japan Society for the Promotion of Science. We are grateful to Sanyo Fine Co., Ltd. for the gift of the chiral epichlorohydrins.

**Supporting Information Available:** Synthesis of PGME amides **ent-9a**, **ent-9b**, **ent-10a**, and **ent-10b**; the experimental details by which the determination of the 1'-configurations of **ent-2a** and **ent-2b** by the PGME method was effected; the structures and pK<sub>i</sub> values of the H<sub>3</sub> receptor antagonists used for the docking simulations; and elemental analysis data of the final compounds. This material is available free of charge via the Internet at <http://pubs.acs.org>.



## References

- (1) (a) Arrang, J.-M.; Garbarg, M.; Schwartz, J.-C. Auto-inhibition of brain histamine release mediated by a novel class ( $H_3$ ) of histamine receptor. *Nature* **1983**, *302*, 832–837. (b) Leurs, R.; Timmerman, H., Eds. *The Histamine H<sub>3</sub> Receptor, a Target for New Drugs*; Elsevier: Amsterdam, 1998. (c) Leurs, R.; Bakker, R. A.; Timmerman, H.; de Esch, I. J. P. The histamine  $H_3$  receptor: from gene cloning to  $H_3$  receptor drugs. *Nat. Rev. Drug Discovery* **2005**, *4*, 107–120. (d) Celanire, S.; Wijtmans, M.; Talaga, P.; Leurs, R.; de Esch, I. J. P. Histamine  $H_3$  receptor antagonists reach for the clinic. *Drug Discovery Today* **2005**, *10*, 1613–1627. (e) Esbenshade, T. A.; Fox, G. B.; Cowart, M. D. Histamine  $H_3$  receptor antagonists: preclinical promise for treating obesity and cognitive disorders. *Mol. Interventions* **2006**, *6*, 77–88. (f) Ali, S. M.; Tedford, C. E.; Gregory, R.; Handley, M. K.; Yates, S. L.; Hirth, W. W.; Phillips, J. G. Design, synthesis, and structure–activity relationships of acetylene-based histamine  $H_3$  receptor antagonists. *J. Med. Chem.* **1999**, *42*, 903–909.
- (2) (a) Klabunde, T.; Hessler, G. Drug design strategies for targeting G-protein-coupled receptors. *ChemBioChem* **2002**, *3*, 928–944. (b) Palczewski, K.; Kumasaka, T.; Hori, T.; Behnke, C. A.; Motoshima, H.; Fox, B. A.; Le Trong, I.; Teller, D. C.; Okada, T.; Stenkamp, R. E.; Yamamoto, M.; Miyano, M. Crystal structure of rhodopsin: a G protein-coupled receptor. *Science* **2000**, *289*, 739–745. (c) Sarramegna, V.; Talmont, F.; Demange, P.; Milon, A. Heterologous expression of G-protein-coupled receptors: comparison of expression systems from the standpoint of large-scale production and purification. *Cell. Mol. Life Sci.* **2003**, *60*, 1529–1546. (d) Schlyer, S.; Horuk, R. I want a new drug: G-protein-coupled receptors in drug development. *Drug Discovery Today* **2006**, *11*, 481–493 and references therein.
- (3) (a) Cherezov, V.; Rosenbaum, D. M.; Hanson, M. A.; Rasmussen, S. G.; Thian, F. S.; Kobilka, T. S.; Choi, H. J.; Kuhn, P.; Weis, W. I.; Kobilka, B. K.; Stevens, R. C. High-resolution crystal structure of an engineered human  $\beta_2$ -adrenergic G protein-coupled receptor. *Science* **2007**, *318*, 1258–1265. (b) Rosenbaum, D. M.; Cherezov, V.; Hanson, M. A.; Rasmussen, S. G.; Thian, F. S.; Kobilka, T. S.; Choi, H. J.; Yao, X. J.; Weis, W. I.; Stevens, R. C.; Kobilka, B. K. GPCR engineering yields high-resolution structural insights into  $\beta_2$ -adrenergic receptor function. *Science* **2007**, *318*, 1266–1273. (c) Rasmussen, S. G.; Choi, H. J.; Rosenbaum, D. M.; Kobilka, T. S.; Thian, F. S.; Edwards, P. C.; Burghammer, M.; Ratnala, V. R.; Sanishvili, R.; Fischetti, R. F.; Schertler, G. F.; Weis, W. I.; Kobilka, B. K. Crystal structure of the human  $\beta_2$  adrenergic G-protein-coupled receptor. *Nature* **2007**, *450*, 383–387.
- (4) (a) Kier, L. B. Molecular orbital calculations of the preferred conformations of histamine and a theory on its dual activity. *J. Med. Chem.* **1968**, *11*, 441–445. (b) Silverman, R. B. *The Organic Chemistry of Drug Design and Drug Action*; Academic Press: San Diego, CA, 2004.
- (5) (a) Kazuta, Y.; Matsuda, A.; Shuto, S. Development of versatile *cis*- and *trans*-dicarbon-substituted chiral cyclopropane units: synthesis of (1*S*,2*R*)- and (1*R*,2*R*)-2-aminomethyl-1-(1*H*-imidazol-4-yl)cyclopropanes and their enantiomers as conformationally restricted analogs of histamine. *J. Org. Chem.* **2002**, *67*, 1669–1677. (b) Kazuta, Y.; Hirano, K.; Natsume, K.; Yamada, S.; Kimura, R.; Matsumoto, S.; Furuichi, K.; Matsuda, A.; Shuto, S. (1*S*,2*S*)-2-(2-Aminoethyl)-1-(1*H*-imidazol-4-yl)cyclopropane, a highly selective agonist for the histamine  $H_3$  receptor, having a *cis*-cyclopropane structure. *J. Med. Chem.* **2003**, *46*, 1980–1988. (c) Watanabe, M.; Kazuta, Y.; Hayashi, H.; Yamada, S.; Matsuda, A.; Shuto, S. The stereochemical diversity-oriented conformational restriction strategy. Development of potent histamine  $H_3$  and/or  $H_4$  receptor antagonists with an imidazolylcyclopropane structure. *J. Med. Chem.* **2006**, *49*, 5787–5796.
- (6) (a) Shuto, S.; Ono, S.; Hase, Y.; Kamiyama, N.; Takada, H.; Yamashita, K.; Matsuda, A. Conformational restriction by repulsion between adjacent substituents of a cyclopropane ring: design and enantioselective synthesis of 1-phenyl-2-(1-aminoalkyl)-*N,N*-diethylcyclopropanecarboxamides as potent NMDA receptor antagonists. *J. Org. Chem.* **1996**, *61*, 915–923. (b) Shuto, S.; Ono, S.; Hase, Y.; Ueno, Y.; Noguchi, T.; Yoshii, K.; Matsuda, A. Synthesis and biological activity of conformationally restricted analogs of milnacipran: (1*S*,1*R*)-1-phenyl-2-[(*S*)-1-aminopropyl]-*N,N*-diethylcyclopropanecarboxamide, an efficient noncompetitive *N*-methyl-D-aspartic acid receptor antagonist. *J. Med. Chem.* **1996**, *39*, 4844–4852. (c) Shuto, S.; Ono, S.; Imoto, H.; Yoshii, K.; Matsuda, A. Synthesis and biological activity of conformationally restricted analogs of milnacipran: (1*S*,2*R*)-1-phenyl-2-[(*R*)-1-amino-2-propynyl]-*N,N*-diethylcyclopropanecarboxamide is a novel class of NMDA receptor channel blocker. *J. Med. Chem.* **1998**, *41*, 3507–3514. (d) Ono, S.; Ogawa, K.; Yamashita, K.; Yamamoto, T.; Kazuta, Y.; Matsuda, A.; Shuto, S. Conformational analysis of the NMDA receptor antagonist (1*S*,2*R*)-1-phenyl-2-[(*S*)-1-aminopropyl]-*N,N*-diethylcyclopropanecarboxamide (PPDC) designed by a novel conformational restriction method based on the structural feature of cyclopropane ring. *Chem. Pharm. Bull.* **2002**, *50*, 966–968 and references therein.
- (7) Ohmori, Y.; Yamashita, A.; Tsujita, R.; Yamamoto, T.; Taniuchi, K.; Matsuda, A.; Shuto, S. A method for designing conformationally restricted analogs based on allylic strain: synthesis of a novel class of noncompetitive NMDA receptor antagonists having the acrylamide structure. *J. Med. Chem.* **2003**, *46*, 5326–5333.
- (8) For examples, see the following: (a) Armstrong, P. D.; Cannon, J. G.; Long, J. P. Conformationally rigid analogs of acetylcholine. *Nature* **1998**, *220*, 65–66. (b) Shimamoto, K.; Ofune, Y. Syntheses and conformational analyses of glutamate analogs: 2-(2-carboxy-3-substituted-cyclopropyl)glycines as useful probes for excitatory amino acid receptors. *J. Med. Chem.* **1996**, *39*, 407–423. (c) Stammer, S. H. Cyclopropane amino acids; 2,3- and 3,4-methanoamino acids. *Tetrahedron* **1990**, *46*, 2231–2254. (d) Martin, S. F.; Dwyer, M. P.; Hartmann, B.; Knight, K. S. Cyclopropane-derived peptidomimetics. Design, synthesis, and evaluation of novel enkephalin analogs. *J. Org. Chem.* **2000**, *65*, 1305–1318. (e) Sekiyama, T.; Hatsuya, S.; Tanaka, Y.; Uchiyama, M.; Ono, N.; Iwayama, S.; Oikawa, M.; Suzuki, K.; Okunishi, M.; Tsuji, T. Synthesis and antiviral activity of novel acyclic nucleosides: discovery of a cyclopropyl nucleoside with potent inhibitory activity against herpes viruses. *J. Med. Chem.* **1998**, *41*, 1284–1298.
- (9) (a) Wong, H. N. C.; Hon, M.-Y.; Tse, C.-Y.; Yip, Y.-C. Use of cyclopropanes and their derivatives in organic synthesis. *Chem. Rev.* **1989**, *89*, 165–198. (b) Singh, V. K.; DattaGupta, A.; Sekar, G. Catalytic enantioselective cyclopropanation of olefins using carbene chemistry. *Synthesis* **1997**, 137–149. (c) Doyle, M. P.; Protopopova, M. N. New aspects of catalytic asymmetric cyclopropanation. *Tetrahedron* **1998**, *54*, 7919–7946. (d) Cossy, J.; Blanchard, N.; Meyer, C. Stereoselective synthesis of cyclopropanes bearing adjacent stereocenters. *Synthesis* **1999**, 1063–1075. (e) *Small Ring Compounds in Organic Synthesis VI*; de Meijere, A., et al., Eds.; Topics in Current Chemistry 207; Springer: Berlin, 1999. (f) Lebel, H.; Marcoux, J.-F.; Molinaro, C.; Charette, A. B. Stereoselective cyclopropanation reactions. *Chem. Rev.* **2003**, *103*, 977–1050. (g) Garcia, P.; Diez, D.; Anton, A. B.; Garrido, N. M.; Marcos, I. S.; Basabe, P.; Urones, J. G. Stereoselective synthesis of cyclopropanols. *Mini-Rev. Org. Chem.* **2006**, *3*, 291–314. (h) Muller, P.; Allenbach, Y. F.; Chappellet, S.; Ghanem, A. Asymmetric cyclopropanations and cycloadditions of dioxocarbenes. *Synthesis* **2006**, *10*, 1689–1696.
- (10) Yabuuchi, T.; Kusumi, T. Phenylglycine methyl ester, a useful tool for absolute configuration determination of various chiral carboxylic acids. *J. Org. Chem.* **2000**, *65*, 397–404.
- (11) For detail of the determination of the 1'-configuration, see Supporting Information.
- (12) The structures and  $pK_i$  values for  $H_3$  receptor of these antagonists are summarized in Table S1 in Supporting Information.
- (13) (a) Rai, B. K.; Tawa, G. J.; Katz, A. H.; Humblet, C. Modeling G protein-coupled receptors for structure-based drug discovery using low-frequency normal modes for refinement of homology models: application to  $H_3$  antagonists. *Proteins* **2010**, *78*, 457–473. (b) Dastmalchi, S.; Hamzeh-Mivehroud, M.; Ghafourian, T.; Hamzeiy, H. Molecular modeling of histamine  $H_3$  receptor and QSAR studies on arylbenzofuran derived  $H_3$  antagonists. *J. Mol. Graphics Modell.* **2008**, *26*, 834–844. (c) Axe, F. U.; Bembenek, S. D.; Szalma, S. Three-dimensional models of histamine  $H_3$  receptor antagonist complexes and their pharmacophore. *J. Mol. Graphics Modell.* **2006**, *24*, 456–464.
- (14) (a) Mobarec, J. C.; Sanchez, R.; Filizola, M. Modern homology modeling of G-protein coupled receptors: which structural template to use? *J. Med. Chem.* **2009**, *52*, 5207–5216. (b) Senderowitz, H.; Marantz, Y. G Protein-coupled receptors: target-based in silico screening. *Curr. Pharm. Des.* **2009**, *15*, 4049–4068. (c) de Graaf, C.; Rognan, D. Customizing G protein-coupled receptor models for structure-based virtual screening. *Curr. Pharm. Des.* **2009**, *15*, 4026–4048. (d) Costanzi, S. On the applicability of GPCR homology models to computer-aided drug discovery: a comparison between in silico and crystal structures of the  $\beta_2$ -adrenergic receptor. *J. Med. Chem.* **2008**, *51*, 2907–2914.
- (15) Thompson, J. D.; Higgins, D. G.; Gibson, T. J. CLUSTAL W. Improving the sensitivity of progressive multiple sequence alignment through sequence weighting, position-specific gap penalties and weight matrix choice. *Nucleic Acids Res.* **1994**, *22*, 4673–4680.
- (16) Levitt, M. Accurate modeling of protein conformation by automatic segment matching. *J. Mol. Biol.* **1992**, *226*, 507–533.
- (17) Lee, C.; Irazarry, K. The GeneMine system for genome/proteome annotation and collaborative data mining. *IBM Syst. J.* **2001**, *40*, 592–603.